Plant Communications
Correspondence

CellPress
Partner Journal

DockingDB: An online reverse-docking database for plant hormone research

Dear Editor,

Phytohormones are pivotal signaling molecules that orchestrate a wide array of physiological and developmental processes in plants (Weyers and Paterson, 2001). Eight major classes of phytohormones, including auxins, cytokinins (CKs), gibberellins (GAs), abscisic acid (ABA), brassinosteroids (BRs), jasmonates (JAs), salicylic acid (SA), and strigolactones (SLs), function through complex interaction networks to regulate plant growth and adaptation. Among these regulatory molecules, CKs constitute a particularly important class of hormones that govern diverse physiological processes. Endogenous CKs predominantly occurs as adenine derivatives characterized by modifications at the N6 position, and the principal bioactive forms includes N6-isopentenyladenine (iP), *trans*-zeatin (tZ), *cis*-zeatin (cZ), and dihydrozeatin (DZ). CK-related compounds also include synthetic analogs, such as 6-benzylaminopurine (BA) and kinetin (Kin) (Sharif et al., 2022), as well as the phenylurea derivatives thidiazuron and diphenylurea (Ha et al., 2012). The CK regulatory network exhibits remarkable functional pleiotropy, and a major challenge remains the comprehensive identification of new components involved in CK signaling, transport, metabolism, and antagonism.

Molecular docking predicts optimal binding poses and estimates binding energies by positioning small molecules within protein binding pockets or active sites (Sousa et al., 2006). Along with molecular dynamics (MD), molecular docking is widely used to predict ligand–receptor interactions. Despite their extensive application in drug discovery, the potential of molecular docking and MD in plant research remains largely unexplored.

To systematically map phytohormone interactomes, we constructed DockingDB, a specialized reverse-docking database that integrate 5,794 experimentally resolved plant protein structures retrieved from the Research Collaboratory for Structural Bioinformatics (RCSB) Protein Data Bank (PDB). This dataset comprises proteins from *Arabidopsis* (37.0%), staple crops (*Triticum aestivum*, 12.1%; *Zea mays*, 8.7%; *Oryza sativa*, 6.4%; *Pisum sativum*, 2.3%; and *Spinacia oleracea*, 1.5%), and other plant species. This curated dataset was automatically preprocessed in DockingDB to generate docking-ready conformations, enabling high-throughput screening of hormone–protein interactions across phylogenetically diverse plant systems.

Developed as an automated extension of UCSF DOCK6 (Allen et al., 2015), DockingDB addresses the scalability limitations of traditional molecular docking by implementing parallelized workflows for plant proteome-scale reverse virtual screening. The pipeline automates preprocessing of input structures through a multistep protocol. Protein structures from the PDB are processed to remove crystallographic waters and heteroatoms; hydrogens are then added, residue are standardized, and charges are assignment using AMBER ff14SB force-field parameters before conversion to MOL2 format. Small molecules are removed from ligand-bound structures before processing, whereas hydrogen-free PDB files are generated in parallel for pocket detection. Pocket prediction uses context-specific strategies: sphgen-based clustering identifies the largest cavity in ligand-free structures, whereas ligand-proximal 8 Å spheres guide pocket definition in ligand-bound structures. These procedures are executed through UCSF Chimera's Python API (Pettersen et al., 2004) to batch-process the retrieved proteins into 18,795 dockable pockets. Ligand preprocessing standardizes PDB, MOL2, and SMILES inputs into canonical MOL2 format by adding hydrogens and calculating AM1-BCC charges, and uses a SMILES-hashed caching system to eliminate redundant docking computations (Figure 1A). This integrated approach enables full automation from raw structural data to dockable complexes (Supplemental Figure 1), substantially increasing throughput relative to manual DOCK6 operations while maintaining high pocket-prediction accuracy against expert-curated benchmarks. DockingDB (https://cbi.gxu.edu.cn/DockingDB) provides reverse-docking results for representative molecules from major phytohormone classes, including CKs (Kin, iP, BA, tZ, cZ, DZ, and diphenylurea), indole-3-acetic acid (IAA, auxin), GA_3, brassinolide (BL), jasmonic acid (JA), and the synthetic SL analog GR24, against the predicted dockable pockets. Users can browse reverse-docking results for each phytohormone across the pockets of each protein structure or search docking results by protein name or PDB ID (Supplemental Figure 2).

Reverse docking of Kin identified known CK receptors and metabolic enzymes among the top-ranked interactions, validating the predictive capacity of the platform. The canonical CK receptor *Arabidopsis* histidine kinase 4 (AHK4, PDB: 3T4S/3T4Q) exhibited strong predicted binding affinities, with Grid scores of −42.24 (rank 60/18,795; top 0.32%) and −41.70 (rank 91/18,795; top 0.48%) across its dimeric binding pockets. Established CK-binding enzymes, including cytokinin oxidase/dehydrogenase (PDB: 5HMR; rank 273; top 1.45%), dehydrogenase (PDB: 1W1O; rank 375; top 2.00%), and oxidase/dehydrogenase (PDB: 2QPM; rank 797; top 4.24%), showed moderate but favorable docking scores, despite potential conformational sampling limitations associated with static crystal structures. Extended screening of additional CK variants revealed conserved low-energy binding pockets across phylogenetically diverse plant proteins, with natural CKs showing stronger average predicted affinities than synthetic analogs, suggesting evolutionary optimization for endogenous ligand recognition. Using the calculated binding energies between CK variants and their cognate receptors as a baseline (Supplemental Table 1), we found that these known interactions consistently ranked among the top 20% of

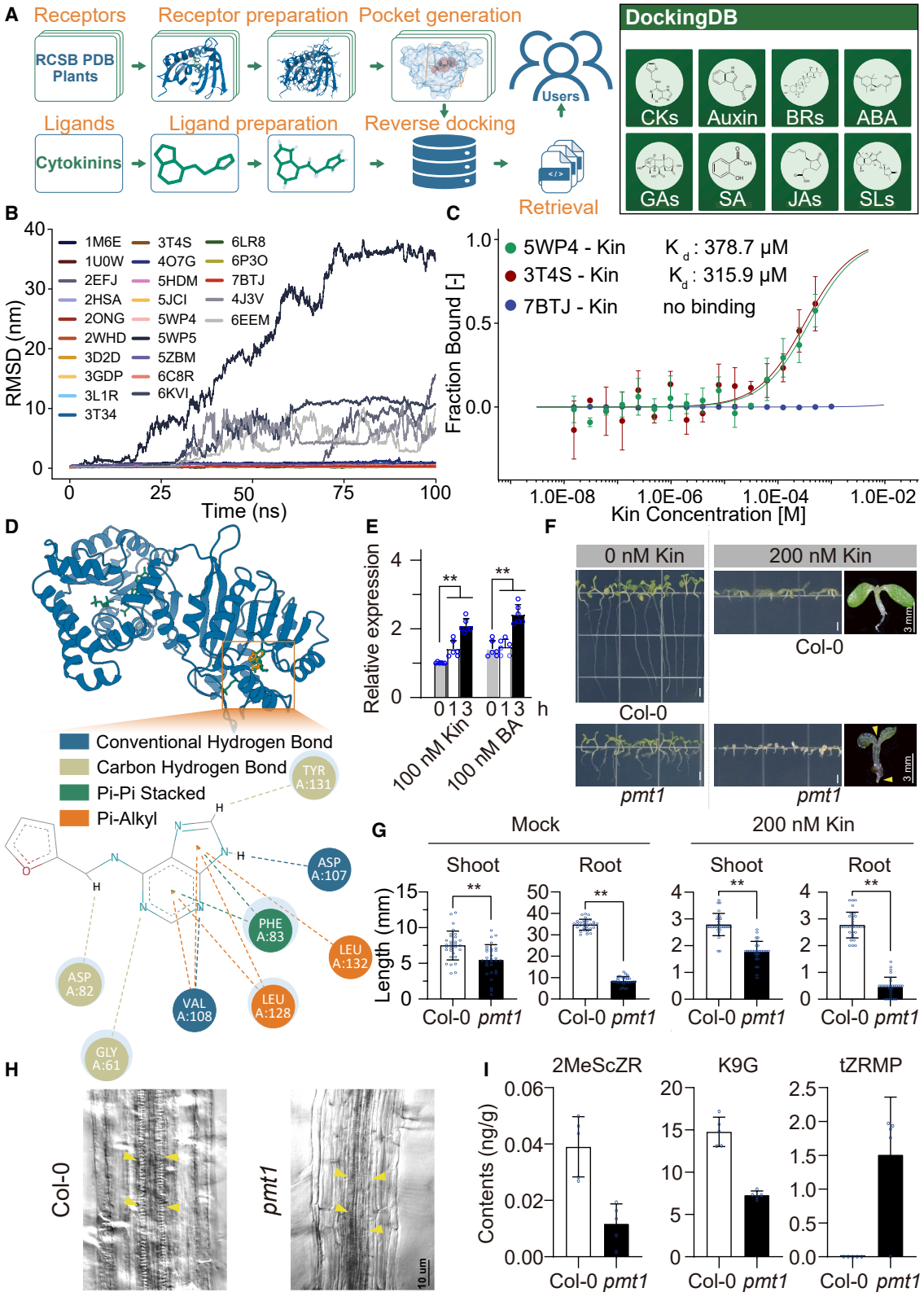

Figure 1. Overview of DockingDB database architecture and functionality and validation of *Arabidopsis* phosphoethanolamine N-methyltransferase 1 (AtPMT1) in cytokinin metabolism and/or signaling.

(A) DockingDB workflow, including protein preparation and pocket generation, ligand preparation, reverse docking, result retrieval, and the DockingDB web interface. The plant protein dataset was retrieved from the Research Collaboratory for Structural Bioinformatics Protein Data Bank (RCSB PDB). After

(legend continued on next page)

hits in DockingDB. Docking results meeting this binding-energy threshold were classified as positive hits, and the corresponding pockets were identified as potential binding sites. To ensure reliability, pockets showing positive docking results with at least six distinct CK molecules were selected, and the associated proteins were categorized as high-confidence candidates (Supplemental Table 2). Based on these criteria, 24 potential Kin-interacting proteins were identified with high confidence and selected for experimental validation (Supplemental Table 3).

To further refine the reverse-docking results, 100-ns MD simulations were performed for the 24 potential Kin-interacting proteins. Thirteen proteins exhibited root-mean-square deviation (RMSD) values that remained consistently below 5 Å after least-squares fitting of the protein backbone (Figure 1B), indicating a higher probability of stable binding with Kin.

Gene fragments encoding the hormone-binding domain of the CK receptor AHK4 (residues 149–418; PDB: 3T4S), together with the genes encoding the 24 potential interacting proteins, were codon-optimized, synthesized, cloned into the pRSFDuet-1 vector, and heterologously expressed in an *Escherichia coli* expression system. After purification by affinity chromatography and gel-filtration chromatography, high-purity protein samples of AHK4 and 19 potential interacting proteins were obtained (Supplemental Figure 3). Microscale thermophoresis (MST) was then used to assess potential interactions. AHK4 (PDB: 3T4S) served as a positive control, with the dissociation constant (K_D) between Kin and AHK4 determined to be 315.9 μM. Among the 19 potential binding proteins, eight interacted with Kin (Figure 1C), with K_D values ranging from 219.7 to 476.6 μM, comparable to that of the positive control (Supplemental Figure 4; Supplemental Table 4).

The binding affinity of iP for the same 19 candidate interacting proteins was also evaluated. MST experiments showed that the eight proteins that interacted with Kin also bound iP. The K_D between iP and AHK4 was 503.4 μM, whereas the K_D values for the eight potential iP-interacting proteins ranged from 288.1 to 733.8 μM (Supplemental Figure 5). Another candidate protein, PsTyDC (PDB: 6EEM), interacted with iP but not Kin (Supplemental Table 5). All Kin- and/or iP-interacting proteins validated by MST were also supported by MD simulations.

We subsequently investigated the biological relevance of AtPMT1, a newly identified CK-interacting protein in *Arabidopsis*. AtPMT1 (PDB: 5WP4) is a phosphoethanolamine N-methyltransferase that catalyzes the methylation of phosphoethanolamine to phosphocholine, a critical step in the conversion of the membrane lipid phosphatidylethanolamine to phosphatidylcholine. AtPMT1 also plays important roles in hydrogen peroxide and auxin homeostasis (Zou et al., 2019). AtPMT1 may associate with CK because the ethanolamine moiety of its isoprene-derived side chain structurally resembles the N6 substituent attached to the purine ring in CK. Docking results revealed multiple interaction types, including conventional hydrogen bonds between AtPMT1 residues Asp107 and Val108 and Kin, as well as carbon–hydrogen bonds between Kin and Gly61, Asp82, and Tyr131 (Figure 1D).

We examined whether *AtPMT1* expression is induced by CK treatment in *Arabidopsis* Columbia-0. *AtPMT1* expression increased after both Kin and BA treatments (Figure 1E), suggesting its involvement in CK metabolism and/or signaling. We then analyzed the phenotype of the *atpmt1* mutant in response to CK treatment. Loss of *AtPMT1* function severely impaired root development (Figures 1F and 1G). Because excessive concentrations of exogenously applied CK can inhibit growth or even cause plant death, the hypersensitivity of the *atpmt1* mutant to 200 nM Kin further supports a role for AtPMT1 in CK metabolism and/or signaling. Notably, the short-root phenotype of *atpmt1* under normal conditions resembled the effect of exogenous CK application. In addition, an increased number of vascular cell files was observed in *atpmt1* roots (Figure 1H), phenocopying the root vascular phenotype of mutants with disrupted CK signaling (Mähönen et al., 2006). These observations led us to hypothesize that CK homeostasis is altered in the *atpmt1* mutant.

We quantified CK levels in the *atpmt1* mutant using targeted liquid chromatography–tandem mass spectrometry (Supplemental Tables 6 and 7) and found that 2-methylthio-*cis*-zeatin riboside and kinetin-9-glucoside were significantly reduced, whereas 9-ribosyl-*trans*-zeatin 5′-monophosphate was upregulated. Together, these changes are consistent with a role for AtPMT1 in CK methylation (Figure 1I). Collectively, these genetic and metabolic analyses suggest that AtPMT1 regulates CK homeostasis, possibly through CK methylation-related processes.

preprocessing and binding-pocket identification, the dataset was subjected to reverse virtual screening against the preprocessed ligand library, and the results were compiled into a report and returned to the user.

(B) Root-mean-square deviation (RMSD) values of kinetin (Kin) with candidate proteins throughout molecular dynamics (MD) simulations. Different candidate proteins are distinguished by lines of different colors, with the corresponding PDB IDs indicated.

(C) Determination of Kin-binding affinities of the positive control (PDB: 3T4S), a newly identified binding protein (PDB: 5WP4), and a non-binding protein (PDB: 7BTJ) by MST.

(D) Structure of AtPMT1 (PDB: 5WP4) in complex with ligands. The protein is shown in cartoon representation. The native ligand in the AtPMT1 structure is highlighted in green, whereas Kin is shown in orange. The two-dimensional interaction diagram below illustrates the key residues involved in Kin binding and the types of interactions formed.

(E) Relative expression of *AtPMT1* in response to CK treatment. Asterisks () indicate statistically significant differences determined by two-way ANOVA ($n = 3$), $p < 0.01$.

(F) Phenotype of the *atpmt1* mutant in response to high concentrations of CK. Scale bar, 3 mm. Yellow arrowheads indicate dying root and shoot apices.

(G) Quantification of shoot and root lengths ($n = 30$). Asterisks (**) indicate statistically significant differences determined by two-way ANOVA ($n = 3$), $p < 0.01$.

(H) Root xylem morphology of the *atpmt1* mutant. Scale bar, 10 μm. Yellow arrowheads indicate xylem files.

(I) CK levels in the *atpmt1* mutant ($n = 5$). 2MeScZR, 2-methylthio-*cis*-zeatin riboside; tZRMP, 9-ribosyl-*trans*-zeatin 5′-monophosphate; K9G, kinetin-9-glucoside.

In summary, the integration of reverse docking, MD simulation, and experimental validation provides a powerful approach for identifying and characterizing novel phytohormone interactors. The development of DockingDB and the insights gained from this study advance our understanding of CK metabolism and signaling, with potential implications for improving crop productivity and stress tolerance.

DATA AND CODE AVAILABILITY

Reverse docking results for representative molecules from major phytohormone classes, including CKs (Kin, iP, BA, tZ, cZ, DZ, and diphenylurea), indole-3-acetic acid (IAA, auxin), GA_3, brassinolide (BL), jasmonic acid (JA), and the synthetic SL analog GR24, against 18,795 dockable pockets are available in DockingDB (https://cbi.gxu.edu.cn/DockingDB). Other datasets supporting the conclusions of this article are included in the supplemental information.

FUNDING

This work was supported by the Guangxi Natural Science Foundation (2024GXNSFGA010003), the Guangxi Science and Technology Major Program (guikeAA23062085), the National Natural Science Foundation of China (U24A20369 and 32270712), the Guangxi Bagui Youth Talent Training Program (to Z.M.), the Guangxi Natural Science Foundation for Distinguished Young Scholars (2020GXNSFFA297007), and the State Key Laboratory for Conservation and Utilization of Subtropical Agro-Bioresources (sklcusa-a02sklcusa-a202306).

ACKNOWLEDGMENTS

We thank Professor Lizhen Tao for kindly providing the *atpmt1* mutant. No conflict of interest declared.

AUTHOR CONTRIBUTIONS

L.-L.C. and Z.M. conceived the project. L.-L.C., Z.M., W.C., and J.-M.S. designed the research and planned the experiments. Y.-X.G., X.-D.X., S.-Y.Y., Y.-H.S., and Y.K. performed the reverse docking, MD simulations, and bioinformatics analyses. F.L., G.X., Y.K., Z.S., Q.Z., Q.F., and J.M. expressed the potential interacting proteins and performed MST. W.C., X.-D.X., and Y.-H.S. performed the genetic validation. All authors participated in discussions and provided intellectual input. F.L., X.-D.X., W.C., Z.M., and L.-L.C. wrote the manuscript, with input from all authors.

SUPPLEMENTAL INFORMATION

Supplemental information is available at *Plant Communications Online*.

Received: September 23, 2025
Revised: February 20, 2026
Accepted: April 27, 2026
Published: April 30, 2026

Correspondence

Yi-Xiong Guo[1,2,5], Fenmei Liu[1,5], Xin-Dong Xu[1,5], Guolyu Xu[1,5], Si-Ying Ye[1], Yan-Han Shao[1], Yanqiong Kong[1], Zihui Su[1], Qiaoqiao Zhao[1], Qiong Fu[1], Jinxue Ma[1], Jia-Ming Song[3,], Wenguo Cai[1,*], Zhenhua Ming[1,*] and Ling-Ling Chen[1,4,*]*

[1]State Key Laboratory for Conservation and Utilization of Subtropical Agro-bioresources, College of Life Science and Technology, Guangxi University, Nanning 530004, China
[2]College of Informatics, Huazhong Agricultural University, Wuhan 430070, China
[3]College of Agronomy and Biotechnology, Southwest University, Chongqing 400715, China
[4]Yazhouwan National Laboratory, Sanya 572025, China
[5]These authors contributed equally
***Correspondence: Jia-Ming Song (jmsong@swu.edu.cn), Wenguo Cai (wcai@gxu.edu.cn), Zhenhua Ming (zhming@gxu.edu.cn), Ling-Ling Chen (llchen@gxu.edu.cn)**
https://doi.org/10.1016/j.xplc.2026.101880

REFERENCES

Allen, W.J., Balius, T.E., Mukherjee, S., Brozell, S.R., Moustakas, D.T., Lang, P.T., Case, D.A., Kuntz, I.D., and Rizzo, R.C. (2015). DOCK 6: Impact of new features and current docking performance. J. Comput. Chem. **36**:1132–1156.

Ha, S., Vankova, R., Yamaguchi-Shinozaki, K., Shinozaki, K., and Tran, L.S.P. (2012). Cytokinins: metabolism and function in plant adaptation to environmental stresses. Trends Plant Sci. **17**:172–179.

Mähönen, A.P., Bishopp, A., Higuchi, M., Nieminen, K.M., Kinoshita, K., Törmäkangas, K., Ikeda, Y., Oka, A., Kakimoto, T., and Helariutta, Y. (2006). Cytokinin signaling and its inhibitor AHP6 regulate cell fate during vascular development. Science **311**:94–98.

Pettersen, E.F., Goddard, T.D., Huang, C.C., Couch, G.S., Greenblatt, D.M., Meng, E.C., and Ferrin, T.E. (2004). UCSF Chimera — a visualization system for exploratory research and analysis. J. Comput. Chem. **25**:1605–1612.

Sharif, R., Su, L., Chen, X., and Qi, X. (2022). Hormonal interactions underlying parthenocarpic fruit formation in horticultural crops. Hortic. Res. **9**:uhab024.

Sousa, S.F., Fernandes, P.A., and Ramos, M.J. (2006). Protein-ligand docking: current status and future challenges. Proteins **65**:15–26.

Weyers, J.D.B., and Paterson, N.W. (2001). Plant hormones and the control of physiological processes. New Phytol. **152**:375–407.

Zou, Y., Zhang, X., Tan, Y., Huang, J.B., Zheng, Z., and Tao, L.Z. (2019). Phosphoethanolamine N-methyltransferase 1 contributes to maintenance of root apical meristem by affecting ROS and auxin-regulated cell differentiation in *Arabidopsis*. New Phytol. **224**:258–273.